Tkachenko Waves in Rapidly Rotating Bose-Einstein Condensates

L. O. Baksmaty, S. J. Woo, S. Choi, and N. P. Bigelow

Department of Physics and Astronomy, and Laboratory for Laser Energetics, University of Rochester, Rochester, New York 14627, USA

(Received 15 July 2003; published 20 April 2004)

We present a mean-field theory numerical study of Tkachenko waves of a vortex lattice in trapped atomic Bose-Einstein condensates. Our results show remarkable qualitative and quantitative agreement with recent experiments at the Joint Institute for Laboratory Astrophysics. We extend our calculations beyond the conditions of the experiment, probing deeper into the incompressible regime where we find excellent agreement with analytical results. In addition, bulk excitations observed in the experiment are discussed.

DOI: 10.1103/PhysRevLett.92.160405 PACS numbers: 03.75.Kk, 32.80.Lg, 67.90.+z, 67.40.Vs

The dynamics of quantized vortices are important in a wide variety of physical phenomena from turbulence to neutron stars, to superconductivity and superfluidity [1]. The broad relevance of this problem is partly responsible for the current interest in vortex lattices in trapped Bose-Einstein condensates (BECs). This system is also attractive because it can easily be manipulated and imaged [2–5] and because the condensate is accurately described within mean-field theory [6]. Until recently much of the progress made in the study of vortex arrays in neutral superfluids was in the context of ^{4}He. This system, however, is notoriously difficult to manipulate and control. Vortex lattices in BECs have thus created an unprecendented opportunity to study vortex matter in detail. This has been recently demonstrated in spectacular experiments at the Joint Institute for Laboratory Astrophysics (JILA) in which Tkachenko waves as well as hydrodynamic shape oscillations were directly observed [4]. In this Letter we present a numerical study of these vortex matter excitations. Our approach has the advantage that it does not require any assumptions about the compressibility or homogeneity of the condensate.

In the limiting case of an incompressible irrotational fluid, Tkachenko waves are transverse vortex-displacement waves traveling in the triangular lattice of vortex lines which constitute the ground state of the rotating superfluid [7,8]. In this idealized situation, the size of the vortex core is infinitesimal and the dynamics of the fluid density may be ignored. For a simple illustration, consider a system of n vortices each of circulation k, in an irrotational, incompressible fluid of density ρ contained by a vessel rotating at angular frequency Ω. Let $\mathbf{v}(\mathbf{r})$ represent the fluid velocity at position $\mathbf{r}$. If the position of the ith vortex is labeled by a complex number z_i, the free energy (f) of the array in a frame rotating at Ω may be written as

$$f = -\frac{\rho k^2}{4\pi}\left[\frac{1}{2}\sum_{i=1}^{n}\sum_{j=1}^{n}\log|z_i - z_j|^2 + \Omega\sum_{i=1}^{n}(1 - |z_i|^2)\right]. \tag{1}$$

Here we ignore the effects of the boundaries and the energy associated with vortex cores [1,8]. By taking into account the irrotational ($\nabla \times \mathbf{v} = 0$) and incompressible ($\nabla \cdot \mathbf{v} = 0$) nature of the fluid, we may derive this expression from the simple classical relation for the energy which in this case is purely kinetic: $f = \rho \int[\frac{1}{2}\mathbf{v}(\mathbf{r})^2 - \Omega(\mathbf{r} \times \mathbf{v}(\mathbf{r}))]d\mathbf{r}$. We can observe from Eq. (1) that the vortex lattice, which represents a local minimum of this free energy, results from a competition between two terms: the logarithmic term which represents the intervortex repulsion and the quadratic rotational term which pulls the vortices towards the center. Tkachenko waves are organized oscillations of the vortex positions about this equilibrium. Microscopically, the vortices precess about their equilibrium position in elliptical orbits against the trap rotation with the major axis perpendicular to the wave propagation. On the macroscopic scale, the array is seen to undergo harmonic distortions which shear the lattice and cause the rotation of the array to alternatively slow down and speed up.

Vortex arrays produced in rapidly rotating trapped BECs depart from this idealized case in two important aspects: the system is significantly compressible and the underlying fluid is inhomogeneous. Because of finite compressibility, it is important to consider the dynamics of the underlying fluid for an accurate treatment. This is especially true in light of recent interest in lattices in the mean-field quantum Hall regime [9,10]. To date, most vortex lattice studies rely on incompressible hydrodynamic approximations [1,8,11]. The hydrodynamic approximation restricts the calculation to long wavelength excitations and the assumption of incompressibility ignores the dynamics of the fluid density. Baym [12] has recently demonstrated the importance of compressiblity to the description of current experimental data. The compressibility of the lattice may be gauged from the ratio ξ^2/ϵ^2. Here ξ and ϵ are the healing length and intervortex distance, respectively. The healing length ξ estimates the size of the vortex core. We define these as $\xi = 1/\sqrt{8\pi na}$ and $\epsilon^2 = 2\pi\hbar/(\sqrt{3}\Omega m)$ [6], where a is the scattering length of the trapped species, n is the density at the center of the condensate, m is the mass of the trapped species, and Ω is the angular frequency of the trap rotation. In this Letter we bypass these familiar approximations by adopting a full numerical approach based on mean-field theory.

As an initial step we must construct the undisturbed vortex array to a high degree of accuracy. We focus on the excitations of triangular vortex arrays with hexagonal symmetry, such as those obtained by recent experiments. We work in a 2D geometry which is achieved by integrating out the axial (z) dependence assumed to be frozen in the ground state of the harmonic oscillator. The coupling constant $g_{3D} = (4\pi a\hbar^2)/m$ is renormalized to a quasi-two-dimensional value $g_{2D} \equiv 2\pi g_{3D}/a_z$, where a_z is the oscillator length along the z axis defined in terms of the axial trapping frequency ω_z by $a_z = \sqrt{\hbar/m\omega_z}$. We note that, owing to the centrifugal reduction in the radial trap frequency ω_r, this is a reasonable assumption at high rotation frequencies where most of our studies take place. More importantly, this quasi-2D "pancake" geometry has been experimentally justified by the high quality of direct images of high [13] and low energy lattice excitations—if the curvature of vortex lines were significant, such imaging would not be possible. According to the $T = 0$ mean-field theory, the condensate wave function $\psi = \psi(\mathbf{r}, t)$ in a frame rotating with angular velocity Ω satisfies

$$i\hbar\frac{\partial\psi}{\partial t} = \left[-\frac{\hbar^2}{2m}\nabla^2 + V(\mathbf{r}) + Ng_{2D}|\psi|^2 - L_z\Omega\right]\psi, \quad (2)$$

where ω_r is the radial trapping frequency, N is the number of trapped atoms, and L_z is the angular momentum operator defined as $-i\hbar\frac{\partial}{\partial\phi}$. The external potential $V(\mathbf{r})$ is defined as $V(\mathbf{r}) = \frac{1}{2}m\omega_r^2 r^2$. The corresponding stationary equation is solved using a steepest descent technique starting from a triangular seed array. We denote the ground state by Φ_0 and define its fluctuation $\delta\Phi_0 = u(\mathbf{r})e^{-i\omega t} - v(\mathbf{r})^* e^{i\omega t}$. Following the Bogoliubov–de Gennes procedure, a first-order expansion around the ground state in terms of $\delta\Phi_0$ then yields the eigenequation for the exciation amplitudes $u_j(\mathbf{r})$ and $v_j(\mathbf{r})$ [6]:

$$\begin{aligned} H_+ v_j - g_{2D}N(\Phi_0^*)^2 u_j &= -\omega_j v_j, \\ H_- u_j - g_{2D}N\Phi_0^2 v_j &= \omega_j u_j, \end{aligned} \quad (3)$$

where $H_\pm = (\hat{h}_\perp \pm \Omega\hat{L}_z + 2g_{2D}N|\Phi_0|^2 - \mu)$, and $\hat{h}_\perp = -\frac{\hbar^2}{2m}\nabla_\perp^2 + \frac{1}{2}m\omega_\perp^2\mathbf{r}^2$ is the single particle x-y Hamiltonian. We solve (3) with finite element methods [14] .

In this treatment we rely on a basic and venerable mathematical principle: that the solution of $\hat{K}v_l = \lambda_l v_l$ is equivalent to minimizing $\lambda(v_l^*, v_l) = \int v_l^* \hat{K} v_l d\mathbf{r} / \int |v_l|^2 d\mathbf{r}$. We solve the variational problem by choosing a trial function in a finite element basis. For this purpose, the domain is broken up into pieces (elements) and on each piece the sought function is approximated by a polynomial. Let v_l^h and λ_l^h be the eigenfunction and its associated eigenvalue in this basis. We employ Hermite cubics on square elements of length h, and on each element we choose the 16 unknowns to be the values of the sought function $(v_l, \partial v_l/\partial x, \partial v_l/\partial x, \partial^2 v_l/\partial x\partial y)$ at each of the four vertices. This choice ensures the continuity of the calculated eigenfunction v_l^h and its derivatives listed above. If the operator $\hat{K}$ is bounded then we can expect that as $v_l^h \to v_l$, $\lambda_l^h \to \lambda_l$. For a finite element space of order $k-1$ it has been proved [14] that $\lambda_l^h - \lambda_l \leq ch^{2(k-m)}$, where c is a constant and m is the order of the differential operator (in this case ∇^2) in $\hat{K}$. This gives a bound on the error of the eigenvalues (λ_l) of the operator $\hat{K}$ due to our projection of the eigenvectors v_l into a finite element subspace. Another source of error arises from the perturbation of the eigenvalue equation [Eqs. (3)] itself due to the projection of the exact ground state Φ_0 onto a finite element subspace. For this error estimate we employ a fundamental inequality of the finite element basis: on each element, $|\Phi_0 - \Phi_0^h| \leq C|\Phi_0|_k h^k$, where C is a constant and $|\Phi_0|_k = \sum_{\beta_1+\beta_2=k} \int |\frac{\partial^k\Phi_0}{\partial x^{\beta_1}\partial y^{\beta_2}}|^2$. To ensure reasonable accuracy, h must be small enough to capture features over the three length scales that characterize the lattice: the Thomas-Fermi radius $R_{TF} = \sqrt{2\mu}$, the healing length ξ, and the intervortex spacing ϵ. This prescription makes the problem very expensive and it was not unusual to obtain sparse matrices of the order $10^5 \times 10^5$. To solve such large eigensystems, we used a variety of numerical libraries and visualization tools [15]. Unless otherwise stated, we express energy, length, and time in the oscillator units $\hbar\omega_r$, $\sqrt{\hbar/m\omega_r}$, and $1/\omega_r$, respectively.

Following Ref. [11], we represent a Tkachenko wave by a complex valued function $D_{n,m}(\mathbf{r}, t) = e^{i\phi}[f_{n,m}^a(r) \times \sin(m\phi - \omega t - \alpha) + if_{n,m}^b(r)\cos(m\phi - \omega t - \alpha)]$. The integer pair (n, m) represents the radial and angular excitation order, $\mathbf{r} = (r, \phi)$, α is an arbitrary phase, and $\{f_{n,m}^a(r), f_{n,m}^b(r)\}$ are real valued functions. The real and imaginary parts of $D_{n,m}$ represent the displacement of a vortex at $\mathbf{r}$ along the x and y axes, respectively, and every vortex moves in an elliptical path.

A significant challenge of comparing our numerical calculation to experiment or to analytical results is the proper identification of the excitations obtained. In our calculation, the degree of freedom is the fluctuation of the field amplitude $\delta\Phi_0$, while in analytical work it is the distortion $D_{n,m}$ of the vortex array that is employed. One approach involves making "movies" of each excitation by using $\delta\Phi_0 = u(\mathbf{r})e^{-i\omega t} - v(\mathbf{r})^* e^{i\omega t}$. In Fig. 1 we show snapshots from two such movies for the $(1, 0)$ and $(2, 0)$ modes and compare them to experimental data. This technique, however, has limitations. Even with a high-resolution movie, the excitations are usually difficult to tell apart by eye, especially as ξ^2/ϵ^2 grows, and also

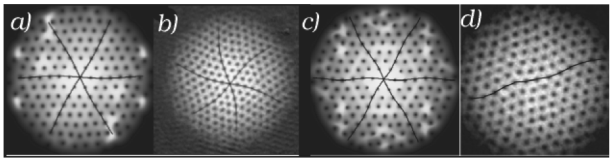

FIG. 1. (a),(b) (1, 0) mode in action: (a) theory and (b) experimental results. The curve is a fitted sine wave with wavelength $1.33R_{\mathrm{TF}}$. (c),(d) (2, 0) mode in action: (c) theory and (d) experimental results. The curves are drawn to guide the eye.

because certain mode branches are very similar in appearance, e.g., the $(n, 0)$ and $(n, 6)$ branches. The experimental identification of the excited mode relies on a sine wave fit to the expanded condenstate. The largely transverse Tkachenko waves become increasingly corrupted by sound waves traveling in the underlying fluid which scatter off the vortices. A more rigorous approach involves extracting $D_{n,m}$ from the fluctuation $\delta\psi$ induced by a particular excitation.

We therefore adopt a quantitative approach based upon determining the instantaneous position of each vortex. A coarse distortion function $D_{n,m}$ can then be constructed by interpolating on the triangular lattice which specifies the ground state. We show a typical result of this calculation in Fig. 2 for a (1, 0) mode in two arrays of similar size but with significantly different ratios of ξ^2/ϵ^2. Along any circle centered at the origin, r is constant and the interpolated distortion $D_{n,m}$ defines a one-dimensional function $d(\phi)$. The Fourier transform of $e^{-i\phi}d(\phi)$ then yields a peak near the value m for the excitation labeled by (n, m). This analysis reveals one important result: the sense of precession of each vortex in an $m \neq 0$ mode may either be with or against the trap rotation. In these modes the sense of precession of a vortex is a function of its radial coordinate only, and along any circle all vortices precess in the same sense. This is a dramatic departure from the ideal situation of an array in a uniform, irrotational, and incompressible fluid. In that case, the vortices precess only against the trap rotation. We note that this has been analytically examined [16].

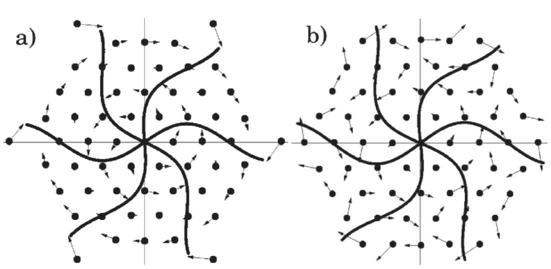

FIG. 2. Calculated distortions of arrays with (a) $\xi^2/\epsilon^2 = 0.007$ and (b) $\xi^2/\epsilon^2 = 0.032$ for a (1, 0) mode. Solid circles: equilibrium vortex positions. Arrows: relative vortex displacement.

Our central result is illustrated by Fig. 3, where we simultaneously make a quantitative comparision of our computations with the JILA experiment [4] and with recent analytic results for a stiff lattice [11]. We focus on the (1, 0) mode. In the stiff regime, which is defined by $\xi^2/\epsilon^2 \to 0$, the speed of sound is much higher than the typical response times of the lattice and the dynamics of the fluid density may be ignored. Here we obtain good agreement with Ref. [11] (which corresponds to the value 1.0 in Fig. 3). We point out that it is not surprising that our energies begin to exceed the analytic prediction as $\xi^2/\epsilon^2 \to 0$. In Ref. [11] the energy of this mode was calculated to first order in ϵ. For small ξ^2/ϵ^2, we consider arrays for which $\epsilon \approx 0.2$ and for which higher order terms in ϵ could be important. At faster rotation and/or lower particle densities the speed of sound lowers, the parameter ξ^2/ϵ^2 increases (abscissa), and we enter the soft regime in which the dynamics of the density is important in the response of the lattice to disturbances. Accordingly, we observe a quantitative deviation from analytic results which is indistinguishable from that experimentally reported [4]. In proportion to this quantitative deviation, we find that the eccentricity of the elliptically polarized vortex oscillations in the Tkachenko wave is reduced and the individual vortex motion becomes almost circular. We illustrate this trend in Fig. 2 [to be compared with Fig. 3(b) in Ref. [11]]. It is noted that the vortex-displacement vectors in Fig. 2(b) have a more significant longitudinal projection than in Fig. 2(a) in which the ratio ξ^2/ϵ^2 is almost an order of magnitude larger.

In the limit of an incompressible fluid, the potential energy of the system is quenched and Tkachenko waves emerge as the only nontrivial class of excitations of a vortex array. However, they are just one of several types of excitations which may occur within the compressible vortex arrays realized in experiments [1]. Of particular interest are the bulk (inertial) modes [12,17], some of which can be very similar in appearance to Tkachenko waves. In Ref. [4] the observation of a rapid mode which

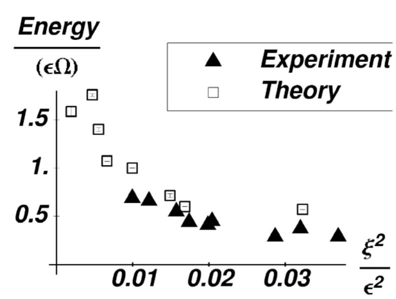

FIG. 3. Energy of the (1, 0) mode versus ξ^2/ϵ^2. In Ref. [11] the energy of this mode is given as $1.43\epsilon\Omega$. The height of the plot symbols represents the error bars for both experiment and theory. The estimate of computational error is described in the text following Ref. [15].

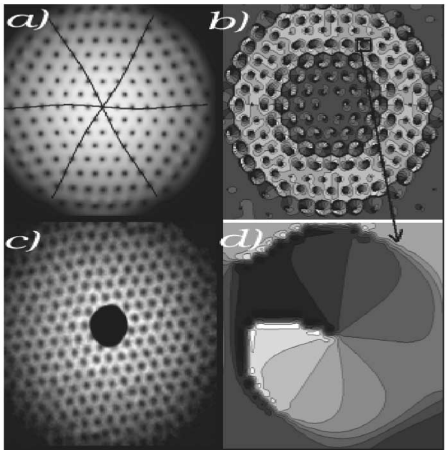

FIG. 4. (a) Bulk (2, 0) mode in action. Overlaid curve is a sine wave of wavelength $1.33R_{\mathrm{TF}}$. (b) Phase plot of $\delta\rho$. Notice the π phase change as a node is radially crossed. (c) Experimental atom removal region [4]. (d) Close-up of (b) on a vortex location. In all phase plots, phase changes from 0 to 2π as one goes from dark to light regions.

is visually indistinguishable from the Tkachenko $(1, 0)$ mode is reported. We also idenitify such a mode at exactly the experimentally reported value of 2.25—this is just the second-order bulk breathing or $(2, 0)$ mode viewed in a rotating frame. This identification also explains the observations made in Ref. [18] in which the experimental procedure of Refs. [4,13] was simulated. There, the frequency of an excited breathing mode continuously changed from $\approx$2.2 to 2.0 with the reduction of atom removal at the center of the trap.

During each half of the oscillatory motion imposed on the vortices by the breathing action in the $(2, 0)$ bulk mode, the transverse (Magnus) force acts in opposite directions. On the microscopic level, elliptical motion of the vortices is observed. Macroscopically, the array twists around the center of rotation like a torsional pendulum as the density breaths radially subject to the coriolis force. We depict this second-order "breathing" mode in Fig. 4(a). Surprisingly, the sine wave radial distortion predicted [11] for the $(1, 0)$ Tkachenko mode is also in very good agreement with this $(2, 0)$ bulk mode. To further illustrate this point, we make use of the complex density fluctuation defined for the nth excitation by [6] $\delta\rho = (\Phi_0^* u_n - v_n^* \Phi_0)$. A casual comparision of the phase of $\delta\rho$ for this mode in Fig. 4(b) with a schematic of the experimental probe in Fig. 4(c) confirms the correct identification of the mode excited in the experiment. A close-up of this phase plot around the position of a vortex is shown in Fig. 4(d). This describes a clockwise elliptical oscillation of the density fluctuation which has a local peak at the vortex core. A similar motion of the vortex at this site is implicated. We predict the existence of third- and fourth-order breathing modes at 2.55 and 3.30, respectively. This is a clear example of how the transverse force and the coriolis force may blur the visual distinction of the largely longitudinal modes from the transverse Tkachenko waves [1]. Our computations have also uncovered a third family of modes restricted to the surface of the condensate and which manifest in the rotating frame as a ring of vortices precessing the stationary ground state [19].

We thank Michael Banks for valuable computing assistance and G. S. Krishnaswami for insightful discussions. We are also grateful to E. A. Cornell for permission to present the JILA data and to J. Anglin and M. Crescimanno for helpful correspondence. This work is supported by DOE, NSF, ARO, and ONR.

[1] E. B Sonin, Rev. Mod. Phys. **59**, 87 (1987).
[2] K. W. Madison, F. Chevy, W. Wohlleben, and J. Dalibard, Phys. Rev. Lett. **84**, 806 (2000).
[3] J. R. Abo-Shaeer, C. Raman, J. M. Vogels, and W. Ketterle, Science **292**, 476 (2001).
[4] I. Coddington, P. Engels, V. Schweikhard, and E. A. Cornell, Phys. Rev. Lett. **91**, 100402 (2003).
[5] V. Bretin, S. Stock, Y. Seurin, and J. Dalibard, Phys. Rev. Lett. **92**, 050403 (2004).
[6] A. L. Fetter and A. A. Svidzinsky, J. Phys. Condens. Matter **13**, R135 (2001).
[7] V. K. Tkachenko, Sov. Phys. JETP **23**, 1049 (1966).
[8] L. J. Campbell, Phys. Rev. A **24**, 514 (1981).
[9] Tin-Lun Ho, Phys. Rev. Lett. **87**, 060403 (2001).
[10] V. Schweikhard, I. Coddington, P. Engels, V. P. Morgendorff, and E. A. Cornell, Phys. Rev. Lett. **92**, 040404 (2004).
[11] J. Anglin and M. Crescimanno, cond-mat/0210063.
[12] G. Baym, Phys. Rev. Lett. **91**, 110402 (2003).
[13] P. Engels *et al.*, Phys. Rev. Lett. **89**, 100403 (2002).
[14] G. Strang and G. Fix, *An Analysis of the Finite Element Method* (Prentice-Hall, Englewood Cliffs, NJ, 1973).
[15] L. O. Baksmaty (to be published).
[16] J. Anglin and M. Crescimanno (private communication).
[17] M. Cozzini and S. Stringari, Phys. Rev. A **67**, 041602(R) (2003); S. Choi, L. O. Baksmaty, S. J. Woo, and N. P. Bigelow, Phys. Rev. A **68**, 031605(R) (2003).
[18] T. P. Simula, A. A. Penckwitt, and R. J. Ballagh, Phys. Rev. Lett. **92**, 060401 (2004).
[19] L. O. Baksmaty, S. J. Woo, S. Choi, and N. P. Bigelow, cond-mat/0310567.